

## Influences of canopy structure and physiological traits on flux partitioning between understory and overstory in an eastern Siberian boreal larch forest

Bao-Lin Xue<sup>a,\*</sup>, Tomo'omi Kumagai<sup>a,b,1</sup>, Shin'ichi Iida<sup>c</sup>, Taro Nakai<sup>d</sup>, Kazuho Matsumoto<sup>a</sup>, Hikaru Komatsu<sup>a</sup>, Kyoichi Otsuki<sup>a</sup>, Takeshi Ohta<sup>e</sup>

<sup>a</sup> Kasuya Research Forest, Kyushu University, Sasaguri, Fukuoka 811-2415, Japan

<sup>b</sup> Department of Civil and Environmental Engineering, PO Box 90287, Duke University, Durham, NC 27708-0287, USA

<sup>c</sup> Department of Soil and Water Conservation, Forestry and Forest Products Research Institute, Tsukuba, Ibaraki 305-8687, Japan

<sup>d</sup> International Arctic Research Center, University of Alaska Fairbanks, PO Box 757340, Fairbanks, AK 99775-7340, USA

<sup>e</sup> Graduate School of Bioagricultural Sciences, Nagoya University, Aichi 464-8601, Japan

### ARTICLE INFO

#### Article history:

Received 23 July 2010

Received in revised form 24 January 2011

Accepted 27 January 2011

#### Keywords:

*Larix*  
Photosynthesis  
Transpiration  
Forest floor  
Multilayer model

### ABSTRACT

Boreal forests play an important role in the global balance of energy and CO<sub>2</sub>. Our previous study of elaborate eddy covariance observations in a Siberian boreal larch forest, conducted both above the forest canopy and at the forest floor, revealed a significant contribution of latent heat flux (*LE*) from the cowberry understory to the whole ecosystem *LE*. Thus, in the present study, we examined what factors control the partitioning of whole ecosystem *LE* and CO<sub>2</sub> flux into the understory and overstory vegetation, using detailed leaf-level physiology (for both understory and overstory vegetation) and soil respiration property measurements as well as a multilayer soil-vegetation-atmosphere transfer (SVAT) model. The modeling results showed that the larch overstory's leaf area index (LAI) and vertical profile of leaf photosynthetic capacity were major factors determining the flux partitioning in this boreal forest ecosystem. This is unlike other forest ecosystems that tend to have dense LAI. We concluded that control of the larch overstory's LAI had a relationship with both the coexistence of the larch with the cowberry understory and with the water resources available to the total forest ecosystem.

© 2011 Elsevier B.V. All rights reserved.

### 1. Introduction

Boreal forests exist in a broad band across the northern hemisphere between the approximate latitudes of 50°N and 70°N. Globally, they account for about 25% of forest areas (Food and Agricultural Organization of the United Nations, 2005). Approximately 34% of boreal forests lie in North America, 22% in Europe to the west of the Urals, and 44% in northern Russia to the east of the Urals (Jarvis et al., 2001). These forests play significant roles in both global and regional climates by masking the high reflectance of snow and partitioning the available energy between sensible and latent heat fluxes (Bonan et al., 1992, 1995; Baldocchi et al., 2000a; Snyder et al., 2004; Bonan, 2008). Although mature boreal forests display low levels of annual carbon gain, such forests, nevertheless, store a large amount of carbon (Dixon et al., 1994; Malhi et al., 1999; Bonan, 2008). Some estimates, using inverse modeling from

the latitudinal distribution of atmospheric CO<sub>2</sub> concentrations, suggest that the boreal forests represent a major terrestrial carbon sink in the northern hemisphere (Tans et al., 1990; Ciais et al., 1995; Bousquet et al., 1999).

However, a clear understanding of how the mass and energy exchange between atmosphere and boreal forests responds to environmental factors has yet to be achieved. This question is the focus of this investigation. It is predicted that boreal deforestation cools global climate by reducing net radiation through the increasing of surface albedo. However, many uncertainties, such as the effect of disturbance and stand age on surface fluxes, still remain (Bonan, 2008). Furthermore, as pointed out by Dolman et al. (2004), inverse atmospheric modeling techniques have produced contrasting results. Some have indicated a large carbon sink capacity for boreal forests (Bousquet et al., 1999), while others have concluded a neutral carbon balance (Rödenbeck et al., 2003), mainly because were constrained by the limitations of available measurements.

Boreal forests are particularly notable for the unique manner in which they store carbon in the soil. This is something that does not occur in other forest biomes. According to Malhi et al. (1999), 84% of the carbon is contained within the soil-based organic matter while the other 16% is contained within the active liv-

\* Corresponding author. Tel.: +81 92 948 3113; fax: +81 92 948 3119.

E-mail addresses: [xuebaolin@forest.kyushu-u.ac.jp](mailto:xuebaolin@forest.kyushu-u.ac.jp), [xuebaolin@qq.com](mailto:xuebaolin@qq.com) (B.-L. Xue).

<sup>1</sup> Present address: Hydrospheric Atmospheric Research Center, Nagoya University, Aichi 464-8601, Japan.

ing biomass in the boreal forests, which largely contributes to the terrestrial carbon sink in the northern hemisphere (Bonan, 2008). This soil carbon storage also makes the boreal forests highly sensitive to global warming because the temperature rise could enhance the decomposition of the soil organic matter and stimulate respiration, and thus release a large amount of CO<sub>2</sub> (see Jarvis et al., 2001). Furthermore, the characteristic sparse overstory and dense understory vegetation of eastern Siberian boreal forests mean that latent heat and CO<sub>2</sub> fluxes at the forest floor become highly significant components of the whole canopy mass and energy exchange rates (Baldocchi and Vogel, 1996; Kelliher et al., 1997, 1999; Hollinger et al., 1998; Ohta et al., 2001; Hamada et al., 2004; Iida et al., 2009). It is of particular note that, since the surface temperature is among the major factors determining mass exchange at the surface and can be impacted by the partitioning of available energy to latent and sensible heat fluxes, thus the latent heat flux from the forest floor surface should be of primary concern.

The goal of this study, therefore, is to understand the energy and mass exchange processes between canopy space, air and understory vegetation in the boreal forest ecosystem. Toward this goal, using a multilayer soil-vegetation-atmosphere transfer (SVAT) model described by Kumagai et al. (2006) and detailed field measurements for flux partitioning conducted by Iida et al. (2009), we examined factors such as the overstory trees' canopy structure and leaf physiological traits to see which factors determine the partitioning of total canopy latent heat and CO<sub>2</sub> fluxes into understory and overstory vegetation. Prior to assessing the effect of the overstory tree characteristics on flux partitioning, the SVAT model was first validated using 10-day period data which was selected from 2-year field measurements conducted in a Siberian boreal larch forest.

## 2. Materials and methods

### 2.1. Site description

The experiment was carried out in an area of light taiga on the west bank of the middle reaches of the Lena River in eastern Siberia (62°15'N, 129°14'E, 220 m a.s.l.), 20 km north of the city of Yakutsk. The area is a continuous permafrost region. Previously, specific climatic data has been gathered for the region covering the period from 1998 to 2006 (Ohta et al., 2008). Here, the mean annual temperature was around -10 °C with a minimum temperature of below -50 °C occurring in mid-winter. During the summer season, the active layers overlying the permafrost thaw. The mean yearly maximum thawing depth has been around 147.0 cm. The mean annual precipitation was around 259.2 mm, but was also highly seasonal, ranging from around 69.0 mm for October–April to around 190.3 mm for May–September (Ohta et al., 2008).

Two stories of vegetation were apparent for the forest of the study site. The dominant overstory species was the deciduous coniferous larch (*Larix cajanderi* Mayr.), having a mean tree height of 20.5 m, a stand density of 808 trees ha<sup>-1</sup>, and a basal area of 27.6 m<sup>2</sup> ha<sup>-1</sup> (Matsumoto et al., 2008). The understory vegetation was very dense and low (<0.1 m), consisting of evergreen cowberry (*Vaccinium vitis-idaea* L.), which provided total ground cover. The leaf area index (LAI) of the larch was determined to be 1.6 and 2.0 by a plant canopy analyzer (LAI-2000, Li-Cor, Lincoln, NE) and the litter trap method (Iida et al., 2009), respectively. The LAI of the cowberry understory was measured by a destructive method and estimated to be 2.1 (Iida et al., 2009).

### 2.2. Meteorological and flux measurements

A 32-m tall tower was constructed at the site for micrometeorological and above-canopy flux measurements. The topography around the tower was almost flat, exhibiting only a slight northward incline. The following instruments were installed at the top of the tower: a solar radiometer (MS402F, EKO, Tokyo, Japan), an infrared radiometer (MS202F, EKO, Tokyo, Japan), a cup-anemometer (AC750, Makino, Tokyo, Japan) and a temperature ( $T_a$ ) and a relative humidity ( $RH$ ) sensor (HMP45D, Vaisala, Helsinki, Finland). To compute the net radiation above the canopy ( $R_n$ ), the upward short-wave and long-wave radiation were measured using a solar radiometer (CM06F, Kipp & Zonen, Delft, Netherlands) and an infrared radiometer installed upside-down (MS201F, EKO, Tokyo, Japan), respectively. Forest floor environmental variables such as  $T_a$ ,  $RH$ , wind speed and net radiation, were also measured, using a  $T_a$  and  $RH$  sensor (HMP45D), a cup anemometer (AC750) and a net radiometer (Q-7, REBS, Seattle, WA), respectively, at a height just above the understory vegetation. Micrometeorological data sets were recorded on a data logger (CR10X, Campbell Scientific, Logan, UT) sampling every 10 s and then producing an average for each 10-min period.

A three-dimensional sonic anemometer with an open-path CO<sub>2</sub>/H<sub>2</sub>O analyzer (LI-7500, Li-Cor, Lincoln, NE) was installed at each position at above ground heights of 32.0 m (WindMaster Pro, Gill, Hampshire, UK) and 3.3 m (R3-50, Gill). Wind speeds and a gas concentration time series were all sampled at 10 Hz (CR5000 data-logger, Campbell Scientific). All variances and covariances required for the eddy covariance flux estimates were computed from a 30-min averaging interval. The wind field coordinates were rotated so that the mean lateral and vertical wind speeds were zero over the 30-min periods. We also applied some corrections for turbulent and scalar readings such as for the effects of density fluctuation (as in Webb et al., 1980) and for the errors from the sonic anemometer angle of attack (as in Nakai et al., 2006). Details regarding turbulent data processing are described elsewhere (Nakai et al., 2006; Iida et al., 2009).

The eddy fluxes, as sensible and latent ( $LE$ ) heat fluxes ( $W m^{-2}$ ) and CO<sub>2</sub> flux ( $F_c$ :  $\mu mol m^{-2} s^{-1}$ ), were observed at the above canopy sampling point and denote the fluxes of the whole ecosystem, consisting of fluxes from/into the larch overstory, the cowberry understory, and the soil. The eddy fluxes observed at the above the forest floor sampling point denote the fluxes from the cowberry and the soil alone. It is noteworthy, since soil evaporation is insignificant compared with the  $LE$  at both the above-canopy position ( $LE_o$ ) and also at the above-forest floor position ( $LE_u$ ) given the very dense cowberry cover, that,  $LE_o - LE_u$  and  $LE_u$  can be considered to represent the transpiration rates from the larch and the cowberry, respectively. It has been reported that the detection of the eddy flux within forest canopies is particularly difficult (see Baldocchi et al., 2000b). We therefore confirmed the validity of the  $LE_u$  by examining the shapes of the power spectra and the co-spectra directly (Iida et al., 2009). Further information on the quality control and the energy closure of the  $LE_o$  and  $LE_u$  are presented in Iida et al. (2009).

The  $F_c$  above the canopy ( $F_{co}$ ) is composed of the net assimilation rates of the larch and the cowberry added to both their autotrophic root respiration rates and to that of soil respiration. We assumed that the contribution of the within-canopy CO<sub>2</sub> storage flux to the net ecosystem CO<sub>2</sub> exchange (NEE) could be neglected because of the low LAI for the larch overstory. Nevertheless, in this study there remained some uncertainty in that  $F_{co}$  could be equal to the NEE. Because of the effect of weak winds and the intermittency of turbulence, some doubt also exists as to whether forest floor CO<sub>2</sub> flux ( $F_{cu}$ ) observations could properly detect CO<sub>2</sub> balance between assimilation and respiration for the within-canopy air. Therefore,

both  $F_{CO}$  and  $F_{Cu}$  may need to be corrected; the latter especially so, but sufficient corrections have not yet been conducted. Therefore, in terms of  $F_c$ , we only compared model outputs for the  $F_{CO}$  data.

We selected 10 experimental days from a wider study period conducted during the growing season spanning from 4 to 23 August in 2005. This period was selected because of the availability of the synchronous data of eddy fluxes, leaf-level physiology and soil respiration and the occurrence of ideal environmental conditions, such as low rainfall, moist soil and day-to-day variations in radiation, temperature and humidity. We compared model outputs and eddy flux data of  $LE_o$ ,  $LE_u$  and the  $F_{CO}$  data, and then, after validation, proceeded to conduct additional examinations of ecosystem productivity partitioning between the larch overstory and the cowberry understory.

### 2.3. Leaf-level physiology and soil respiration parameters

Leaf gas exchange measurements for sunlit leaves at the top to middle parts of three larch overstory were conducted on four measurement days, selected between 24 June and 2 September 2005, using a portable IRGA (LI-6400, Li-Cor) (Maksimov et al., 2006) and for seven cowberry understory branches (Maksimov et al., unpublished data). The main leaf-level physiological parameters, i.e., the maximum carboxylation rate when ribulose biphosphate (RuBP) is saturated ( $V_{cmax}$ :  $\mu\text{mol m}^{-2} \text{s}^{-1}$ ) and the potential rate of whole-chain electron transport ( $J_{max}$ :  $\mu\text{mol m}^{-2} \text{s}^{-1}$ ), were computed for both the larch overstory and the cowberry understory from the assimilation  $-\text{CO}_2$  concentration within stomatal cavity relationships (i.e.,  $A-C_i$  curve), which was derived from the *in situ* gas exchange measurements. To model  $\text{CO}_2/\text{H}_2\text{O}$  exchange between the forest and the atmosphere and to compare the model outputs and the flux data, we estimated  $V_{cmax}$  and  $J_{max}$  in August by interpolating and averaging the data from the four leaf gas exchange measurement days. As a result, we obtained a  $V_{cmax}$  at 25 °C ( $V_{cmax,25}$ ) of 49.1  $\mu\text{mol m}^{-2} \text{s}^{-1}$  for the larch (Maksimov et al., 2006) and 30  $\mu\text{mol m}^{-2} \text{s}^{-1}$  for the cowberry (Maksimov et al., unpublished data) and could assume  $J_{max} = 2 V_{cmax}$  for both species (see Wullschleger, 1993). Another important ecophysiological parameter, Ball-Berry stomatal conductance model slope ( $m_L$ : Ball et al., 1987; Collatz et al., 1991), has been reported to vary from about 7 to 10 corresponding to environmental factors (see Baldocchi et al., 2000a). The value of  $m_L$  in this study was assumed to be 7.0, which is similar to the value used by Baldocchi and Meyers (1998) to compute the boreal forest canopy fluxes under the consideration of plausible  $LE_o$  responses.

The  $\text{CO}_2$  efflux from the soil surface was measured during the period from 1 May to 14 July and from 20 July to 25 September 2005 using an automatic closed chamber measurement at four points 25 m northwest from the tower (Kononov et al., 2006). For each chamber, this measurement system consisted of a control unit, four chambers, and soil temperature ( $T_{soil}$ : °C) and moisture sensors placed at a 5-cm depth. These were operated hourly. The soil  $\text{CO}_2$  efflux data were averaged over the four points for each measurement hour and this was regarded as the hourly value of soil respiration rate ( $R_{soil}$ ). In our SVAT model,  $R_{soil}$  is expressed as a power function given by:

$$R_{soil} = R_{soil,0} Q_{10}^{T_{soil}/10} \quad (1)$$

where  $R_{soil,0}$  and  $Q_{10}$  are the fitted parameters representing soil respiration at 0 °C and a rate of increase when  $T_{soil}$  increases by 10 °C, respectively. The parameters  $R_{soil,0}$  and  $Q_{10}$  were estimated to be 1.1 and 4.4, respectively, using least square regression analysis ( $R^2 = 0.81$ ) (Kononov et al., 2006).

### 2.4. SVAT model description

The SVAT model (Kumagai et al., 2006) used in this study consists of three submodels: (1) a model for energy and radiation conservation, (2) an ecophysiological model for stomatal opening and carbon assimilation, and (3) a model for turbulent diffusion. In all computations, the canopy is divided into 50 layers, and all equations in this model are solved at each layer. Note that in the present model, the lowest layer in the canopy was devoted to computing the above submodels (1)–(3) for the cowberry understory only. In other words, for the cowberry understory, assimilation, transpiration and energy exchange occur within this layer having an extremely high leaf area density (LAD). Although a previous study, Kumagai et al. (2006), provided detailed information, a brief review and a description of this modeling scheme together with explanations regarding functions additional to the model, are presented below for completeness.

#### 2.4.1. Radiative transfer and energy balance at both leaf and soil surface levels

When considering the leaf-scale energy balance together with photosynthesis within a forest canopy, the radiative transfer through the canopy must be determined. Then, direct beam and diffuse irradiance must be considered separately due to their different attenuations in the canopy. The probability of no contact within a canopy layer for beam irradiance ( $P_b$ ) needs to be formulated for describing the direct irradiance transfer within the canopy. This formulation includes the leaf area density ( $a_{leaf}$ ), the beam extinction function of solar elevation and the leaf angle distribution within a given layer (see Goudriaan, 1977).

Native vegetation has clumped foliage. This is especially the case for conifers as their needles are organized onto shoots. In this study's model, we incorporate a clumping factor ( $\Omega$ ) in the  $P_b$  equation by replacing  $a_{leaf}$  with  $\Omega a_{leaf}$ , where  $\Omega$  is the function of the solar zenith angle ( $\psi$ ) (see Campbell and Norman, 1998):

$$\Omega(\psi) = \frac{\Omega(0)}{\Omega(0) + (1 - \Omega(0))\exp(-2.2\psi^q)} \quad (2)$$

where  $\Omega(0)$  is the clumping factor when looking up out of the canopy toward the zenith,  $q$  is given by  $3.80 - 0.46D_{crown}$ , where  $D_{crown}$  is the ratio of crown depth to crown diameter, and is considered as 1 and 3.34 when  $q$  is less than 1 and more than 3.34, respectively. The probability of no contact within a canopy layer for diffuse irradiance ( $P_d$ ) is calculated by integrating  $P_b$  over the solid angles of the sky hemisphere.

In this study, above-canopy diffuse solar radiation ( $R_{sd}$ :  $\text{W m}^{-2}$ ) was not measured, and thus we assumed the following equations to estimate  $R_{sd}$  from observed global solar radiation ( $R_s$ :  $\text{W m}^{-2}$ ):

$$R_{sd} = \frac{0.3 - 0.3\tau^m}{0.3 + 0.7\tau^m} R_s \quad (3)$$

where  $m$  is the optical air mass number that depends upon the altitude of the site and  $\psi$ ,  $\tau$  is the atmospheric transmittance function of  $m$ ,  $\psi$  and observed  $R_s$  (see Campbell and Norman, 1998). Downward and upward long-wave radiation ( $R_L$ ) transfer within a canopy follows theories of diffuse irradiance transfer. However, it must be noted that  $R_L$  is emitted from any plant body within the canopy.

Both direct and diffuse solar radiation can be further divided into photosynthetic active radiation (PAR) and near-infrared radiation (NIR) according to their different absorption by leaves. Fortunately, approximately half the  $R_s$  over the canopy is in the form of PAR while the other half is in the form of NIR, enabling estimates of  $R_s$  penetration inside the canopy. The absorbed PAR or NIR within a canopy layer between  $z$  (the height from the ground) and  $z + \Delta z$ ,

$\Delta S$ , is defined as:

$$\Delta S_b = (1 - \eta - \xi)(1 - P_b)S_b(z + \Delta z) \quad (4)$$

$$\Delta S_d^\downarrow = (1 - \eta - \xi)(1 - P_d)S_d^\downarrow(z + \Delta z) \quad (5)$$

$$\Delta S_d^\uparrow = (1 - \eta - \xi)(1 - P_d)S_d^\uparrow(z) \quad (6)$$

where  $\eta$  and  $\xi$  are the leaf transmissivity and reflectivity, respectively, for PAR or NIR, and  $S$  is PAR or NIR at the given height. The subscripts  $b$  and  $d$  denote the direct beam and diffuse irradiation, respectively, and superscript arrows denote the direction of the irradiation. Because  $P_b$  and  $P_d$  are complex functions of the leaf area density, leaf angle distribution and foliage clumping factor within a given canopy layer and the solar geometric direction (see Kumagai et al., 2006), Eqs. (4)–(6) are not readily solved. The total absorbed solar radiation within the canopy layer is then calculated as the sum of the absorbed PAR and NIR, both of which are calculated by Eqs. (4)–(6). Sunlit leaves receive the beam and the upward and downward diffuse radiation, while shaded leaves only receive the upward and downward diffuse radiation. Therefore, the irradiance absorption and energy balance need to be computed separately for the sunlit and shaded leaves (see Kumagai et al., 2006).

The energy balance at the soil surface for computing  $T_{soil}$ , is expressed by:

$$R_{sab,soil} + R_{L,down}(0) - \varepsilon_s \sigma (T_{soil} + 273)^4 = G_{soil} + LE_{soil} + H_{soil} \quad (7)$$

where  $R_{sab,soil}$  is the total  $R_s$  absorbed by the soil surface,  $R_{L,down}(0)$  is the downward  $R_L$  at  $z=0$ ,  $\varepsilon_s$  is the soil emissivity,  $\sigma$  is the Stefan–Boltzmann constant ( $5.67 \times 10^{-8} \text{ W m}^{-2} \text{ K}^{-4}$ ), and  $LE_{soil}$  and  $H_{soil}$  are latent and sensible heat fluxes at the soil surface, respectively.  $LE_{soil}$  and  $H_{soil}$  are the functions of  $T_{soil}$ , as described by the products of the transport conductance and the concentration difference. In addition, the soil surface moisture availability was also used for the  $LE_{soil}$  computation (see Kumagai et al., 2006).  $G_{soil}$  is soil heat storage, assumed to be  $G_1 R_{sab,soil} \sin[2\pi(t - G_2)/24] + G_3$ , where  $t$  is the hour of the day and  $G_1$ ,  $G_2$  and  $G_3$  are fitting parameters.

#### 2.4.2. Leaf-level physiological functions

The leaf-level scalar source strengths, i.e. leaf sensible heat ( $H_l$ :  $\text{W m}^{-2}$ ), transpiration ( $E_l$ :  $\text{kg m}^{-2} \text{ s}^{-1}$ ) and photosynthesis rate ( $A_l$ :  $\mu\text{mol m}^{-2} \text{ s}^{-1}$ ) are derived from physiological controls using:

$$H_l = 2m_a c_p g_{ah} (T_l - T_a) \quad (8)$$

$$E_l = m_e \frac{g_{aw} g_{sw}}{g_{aw} + g_{sw}} \frac{e_{sat}(T_l) - e}{p_a} \quad (9)$$

$$A_l = g_{ac} (C_a - C_s) \quad (10)$$

$$A_l = g_{sc} (C_s - C_i) \quad (11)$$

where  $m_a$  and  $m_e$  are the molecular weights of air and water ( $\text{kg mol}^{-1}$ ), respectively,  $e_{sat}(T_l)$  and  $e$  is the saturation vapor pressure at leaf temperature ( $T_l$ ) and the atmospheric vapor pressure (Pa), respectively,  $p_a$  is the atmospheric pressure (Pa), and  $C_s$ ,  $C_a$  and  $C_i$  are the  $\text{CO}_2$  concentrations ( $\mu\text{mol mol}^{-1}$ ) of air inside and outside the laminar boundary layer of leaves and within the stomatal cavity, respectively.  $g_{ah}$ ,  $g_{aw}$  and  $g_{ac}$  are the boundary layer conductances for heat, water vapor and  $\text{CO}_2$  ( $\text{mol m}^{-2} \text{ s}^{-1}$ ), respectively, calculated according to Campbell and Norman (1998).

$g_{sw}$  and  $g_{sc}$  are the stomatal conductances for water vapor and  $\text{CO}_2$  ( $\text{mol m}^{-2} \text{ s}^{-1}$ ), respectively.  $g_{sc}$  is linked to  $A_l$ , the relative humidity of air inside the boundary layer of a leaf ( $h_s$ ) and  $C_s$ , as described by Ball et al. (1987) and Collatz et al. (1991), and is given by:

$$g_{sc} = m_L \frac{A_l h_s}{C_s} + b_L \quad (12)$$

where  $m_L$  and  $b_L$  are the slope and intercept, respectively, and were obtained by linear regression analysis of data from leaf-level gas exchange measurements.  $g_{sw}$  is obtained from  $g_{sw} = 1.6 g_{sc}$ , where 1.6 is the ratio of diffusivities of water vapor and  $\text{CO}_2$  in air (von Caemmerer and Farquhar, 1981).

$A_l$  was computed using the biochemical model of Farquhar et al. (1980) and Collatz et al. (1991) as a minimum value of the gross rate of photosynthesis limited by the rate of RuBP regeneration through electron transport ( $J_E$ ), RuBP carboxylase-oxygenase (Rubisco) activity ( $J_C$ ) and the export rate of synthesized sucrose ( $J_S$ ), as:

$$A_l = \min\{J_E, J_C, J_S\} - R_d \quad (13)$$

where  $R_d$  is the respiration rate during the day but in the absence of photorespiration. The formulation and parameterization of  $J_E$ ,  $J_C$ ,  $J_S$  and  $R_d$  as a function of PAR absorbed by the leaf,  $\text{CO}_2$  concentration within the stomatal cavity and leaf temperature is used from Farquhar et al. (1980), Farquhar and Wong (1984), Collatz et al. (1991) and de Pury and Farquhar (1997). The photosynthesis model constants can be determined according to Badger and Collatz (1977), Farquhar et al. (1980), von Caemmerer et al. (1994) and de Pury and Farquhar (1997). The  $V_{cmax}$  and the  $J_{max}$  used in these calculations are expressed as non-linear functions of temperature using values at  $25^\circ\text{C}$  ( $V_{cmax,25}$  and  $J_{max,25}$ , respectively); the formulations of which are given in de Pury and Farquhar (1997). In addition,  $R_d$  is expressed as a non-linear function of temperature using  $R_d$  at  $25^\circ\text{C}$  ( $R_{d,25}$ ), which was assumed to be linearly related to  $V_{cmax,25}$  (as in Collatz et al., 1991). Practically, both  $J_{max,25}$  and  $R_{d,25}$  are related to  $V_{cmax,25}$ , and hence,  $V_{cmax,25}$  is the key parameter in the leaf photosynthesis model.

#### 2.4.3. Scalar transport

The scalar continuity and turbulent flux equations are obtained by assuming a steady state planar-homogeneous and high Reynolds and Peclet numbers flow, and by applying time and horizontal averaging (see Katul and Albertson, 1999). In the scalar continuity equations, the source (or sink) terms, due to mass release (or uptake) by the ensemble of leaves within the averaging plane, are given by:

$$S_T = \frac{1}{\rho_a c_p} (H_{lsl} a_{sl} + H_{lsh} a_{sh}) \quad (14)$$

$$S_q = \frac{1}{\rho_a} (E_{lsl} a_{sl} + E_{lsh} a_{sh}) \quad (15)$$

$$S_c = -(A_{lsl} a_{sl} + A_{lsh} a_{sh}) \quad (16)$$

where  $S_T$ ,  $S_q$  and  $S_c$  are the source strengths for heat ( $\text{K s}^{-1}$ ), water vapor ( $\text{kg kg}^{-1} \text{ s}^{-1}$ ) and the  $\text{CO}_2$  concentration ( $\mu\text{mol m}^{-3} \text{ s}^{-1}$ ), respectively,  $\rho_a$  is the density of air ( $\text{kg m}^{-3}$ ),  $c_p$  is the specific heat of air at constant pressure ( $\text{J kg}^{-1} \text{ K}^{-1}$ ), and  $a$  denotes  $a_{leaf}$ . Subscripts  $sl$  and  $sh$  denote the sunlit and shaded leaves, respectively. The turbulent flux equations include unknowns requiring closure approximations for flux transport and pressure scalar gradient covariance as described by Mellor (1973).

To solve the scalar continuity and turbulent flux equations, the vertical wind profiles and other canopy turbulence statistics were derived using the second-order closure model formulated by Wilson and Shaw (1977). Using the measured wind profile and logarithmic law, the momentum roughness length and zero-plane displacement were determined as  $0.15h$  and  $0.36h$ , respectively (where  $h$  is the canopy height) (see Nakai et al., 2008). Note that these values were used to adjust the wind speed measured at the top of the tower to the actual friction velocity. Boundary conditions were specified in accordance with Katul and Albertson (1999), and the closure constants given by Wilson and Shaw (1977), Watanabe (1993) and Katul and Albertson (1999) were used. To solve the

**Table 1**  
Major parameters used for model validation.<sup>a</sup>

Parameter	Value	Units
Latitude	62.4N	degrees
Longitude	129.6E	degrees
Altitude	220	m
$h$	21	m
LAI for larch,	1.6	$\text{m}^2 \text{m}^{-2}$
LAI for cowberry	2.1	$\text{m}^2 \text{m}^{-2}$
Leaf characteristic dimension	0.01	m
$\Omega(0)$	0.5	–
$V_{\text{cmax},25}$ at the top of the canopy for larch	49.1	$\mu\text{mol m}^{-2} \text{s}^{-1}$
$V_{\text{cmax},25}$ for cowberry	28	$\mu\text{mol m}^{-2} \text{s}^{-1}$
$J_{\text{max}}$ for larch and cowberry	$2 V_{\text{cmax}}$	$\mu\text{mol m}^{-2} \text{s}^{-1}$
$R_d$ for larch and cowberry	$0.015 V_{\text{cmax}}$	$\mu\text{mol m}^{-2} \text{s}^{-1}$
$m_L$	7	–
$b_L$	0.01	$\text{mol m}^{-2} \text{s}^{-1}$
$R_{\text{soil},0}$	1.1	$\mu\text{mol m}^{-2} \text{s}^{-1}$
$Q_{10}$	4.4	–

<sup>a</sup> Symbols are represented in text.

second-order closure model, we used the numerical scheme as described by Katul and Albertson (1998, 1999).

### 2.5. Model computations

The SVAT model in this study was parameterized by independently collected ecophysiological measurements and was not calibrated or parameterized by canopy-level flux measurements. Table 1 summarizes the major parameters used for model validation. After model validation using the canopy flux measurement, this model could be used to examine how the matter fluxes above the forest ecosystems were generated, and thus elucidate how the canopy structure and physiological traits control the latent heat and  $\text{CO}_2$  exchange between the larch and the cowberry vegetation and the atmosphere. For this purpose, we conducted three types of numerical experiments as follows.

The leaf nitrogen per unit area ( $N_a$ ) is generally correlated with the light level environment, and, as a result, its vertical distribution within the canopy is generally related to cumulative LAI profiles and light attenuation coefficients (as in Hirose and Werger, 1987). Variation in  $V_{\text{cmax},25}$  can also be explained well by  $N_a$  (as demonstrated in Niinemets and Tenhunen, 1997). Thus, the suggestion that  $V_{\text{cmax},25}$  decreases with decreasing canopy height is a plausible and realistic assumption. For simplification, a linear relationship between  $V_{\text{cmax},25}$  and the canopy height can therefore, be assumed. The first numerical experiment was a model validation using all the measured LAI and ecophysiological parameters (see Table 1). Furthermore, to examine the effect of the distribution of LAI on the canopy flux in the assumption of an even distribution of LAI, we simulated three additional cases: an even LAD distribution (Case 1), the maximum LAD occurring at the upper part of canopy (Case 2) and the maximum LAD occurring at the lower part of canopy (Case 3) (Fig. 1). Note that the LAD distribution of the cowberry understory was assumed to have an even value of  $5.0 \text{ m}^2 \text{ m}^{-3}$  ( $= [2.1 \text{ m}^2 \text{ m}^{-2} : \text{LAI for the cowberry}] / [h/50 \text{ m} : \text{the calculation of the layer's thickness}]$ ) at the lowest layer in the canopy. However, this is not shown in Fig. 1.

Then, we investigated how the LAI of the larch overstory alters both the above-canopy flux and the flux partitioning between the larch overstory and the cowberry understory. The final numerical experiment investigated the impact of the vertical gradient of  $V_{\text{cmax},25}$  in the larch overstory crowns on the fluxes from the larch and the cowberry. This impact was thought to differ in accordance with the overstory LAI. Thus some interaction between the impacts of the vertical gradient of  $V_{\text{cmax},25}$  and the overstory LAI must be considered in this final numerical experiment.

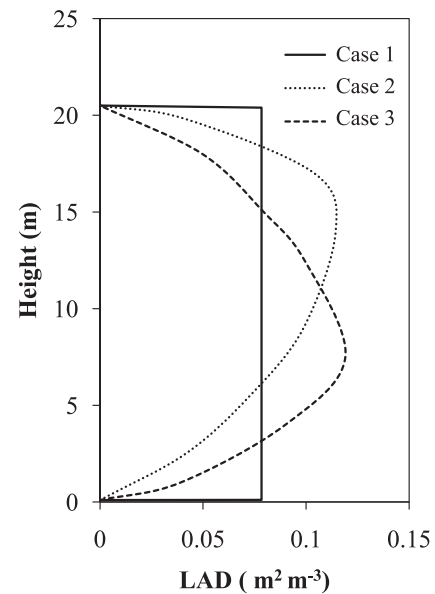


**Fig. 1.** Vertical distributions of leaf area density (LAD) of the larch overstory for Cases 1, 2 and 3 (see text). The LAD of the cowberry understory was assumed to be  $5.0 \text{ m}^2 \text{ m}^{-3}$  at the lowest layer of 0–0.4 m height (not shown here).

## 3. Results and discussion

### 3.1. Model validation and impact of within-canopy leaf area density distribution on flux calculations

The SVAT model clearly reproduced the time series of  $R_n$  (Fig. 2a), showing its ability to synthesize the partitioned canopy transport of energy between the above-canopy and the forest floor. Overall, the calculated  $LE_o$  and  $LE_u$  captures the canonical form of the measured values (Fig. 2a). While there are some discrepancies between calculated and measured  $LE_o$  in the afternoon, the model essentially well represents the measured  $LE_u$  throughout the whole day. Results for both  $LE_o$  and  $LE_u$  for Cases 1–3 are also shown in Fig. 2. The  $LE_o$  in Case 2 was the largest of these because, in this case, leaves concentrated on the upper part of the canopy provided a strong  $LE$  source for the upper canopy (Fig. 2b). Case 3 had its strongest source in the lower part of the canopy, and Case 1 had its strongest source close to the ground. Case 1 had the largest LAD near the ground of all the three cases (Fig. 2b). These results imply that the  $LE$  source strength within a canopy corresponds to the LAD distribution.

For the following experiments, since the difference in  $LE$  calculations between Cases 1 and 3 was small, we used Case 1 where an even LAD distribution was assumed. Fig. 3 shows further comparisons of calculated  $LE_o$  and  $LE_u$  for Case 1 against measurements. A significant ( $t$ -test,  $P < 0.005$ ) but small (20% of the mean) difference existed between the modeled and the measured  $LE_o$ , and the slope and the intercept of the regression line were close to unity and zero, respectively, with a strong correlation ( $y = 1.06x + 9.61$ ,  $R^2 = 0.75$ ) (Fig. 3a). No significant difference between the modeled and the measured  $LE_u$  was observed ( $t$ -test,  $P = 0.83$ ) (Fig. 3b).

As supplementary analyses, we computed the  $F_c$  from the whole canopy ( $F_{co}$ ), the understory vegetation ( $F_{cu}$ ), and the soil surface ( $R_{soil}$ ) for Cases 1–3 (Fig. 4). From the morning until around noon, there was an apparent good fit between modeled and measured  $F_{co}$ . However, a very large discrepancy was apparent for this value for the afternoon to night period (Fig. 4a). Assuming autotrophic leaf, branch and stem respirations to be small compared with  $R_{soil}$ , the differences between  $R_{soil}$  and  $F_{co}$  and between  $R_{soil}$  and  $F_{cu}$  will denote the approximate gross assimilation rates ( $G_p$ ) for the larch

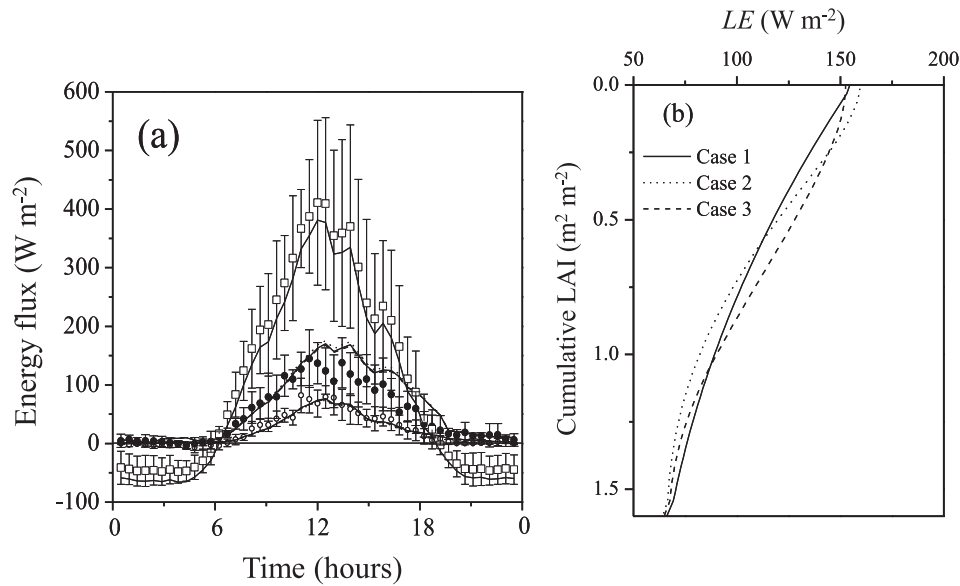


**Fig. 2.** (a) Average temporal variations in measured above-canopy net radiation ( $R_n$ ) (open squares), latent heat flux ( $LE$ ) from whole canopy (solid circles) and understory vegetation (open circles) and simulated  $R_n$  and  $LE$  against each for Cases 1, 2 and 3 (lines). For reference one standard deviation of the measured binned  $LE$  is also shown. (b) Vertical profiles of the average  $LE$  around noon (1100–1300 LT) as a function of cumulative leaf area index (LAI) of overstory vegetation modeled from Cases 1, 2 and 3.

overstory plus cowberry understory and for the cowberry alone, respectively (Fig. 4a). Daily integrations of  $G_p$  for the larch and for the cowberry were almost identical. The effects of the LAD distribution on the  $F_{CO}$  were apparently larger than those on the  $LE_o$  (Figs. 4a and b). Similar to the  $LE$  cases, the strongest  $CO_2$  sink position for each case was located at the upper part of canopy in Case 2, the lower part of canopy in Case 3 and near the forest floor in Case 1 (Fig. 4b). The LAD distribution of the overstory vegetation had little impact upon  $F_{Cu}$  and  $R_{soil}$  (Fig. 4a).

It should be noted that although the  $R_{soil}$  was extremely high (Fig. 4a), this is reasonable considering the anomalous parameters of  $R_{soil,0}$  and  $Q_{10}$ , which were estimated from observation under the exceptionally wet conditions of the period 20 July–25 September 2005 (see Kononov et al., 2006). Further comparison of modeled and measured  $F_{CO}$  is shown in Fig. 5. This indicates that the modeled values fitted the measured values well when the  $F_{CO}$  values were highly negative, but not when  $F_{CO}$  values were around zero or into the positive range. Thus, we deduced that the  $F_{CO}$

during afternoon and nighttime conditions tended to be underestimated for the study site probably because of stable atmospheric and low wind conditions (see Pattey et al., 2002). Note that the statistical parameters of the comparisons between modeled and measured  $F_{CO}$  and  $LE_o$  for the model validation are also presented in Table 2.

Many studies have investigated the contribution of  $LE_u$  to  $LE_o$  in boreal forests (Baldocchi and Vogel, 1996; Kelliher et al., 1997, 1998; Constantin et al., 1999; Ohta et al., 2001; Hamada et al., 2004; Iida et al., 2009). The estimates for  $LE_u$ 's contribution to  $LE_o$  have varied widely, from 10% to 60%. In the 2-year observation period of our study (Iida et al., 2009), the proportion of  $LE_u$  to  $LE_o$  had a seasonal trend with a flat-bottomed U-shape during the growing season from 4 May to 30 September, and its mean value reaching over 50% from 1 June to 31 August, including the computation period of this study. We emphasize that the SVAT model in this study successfully recreated this proportion and its diurnal changes.

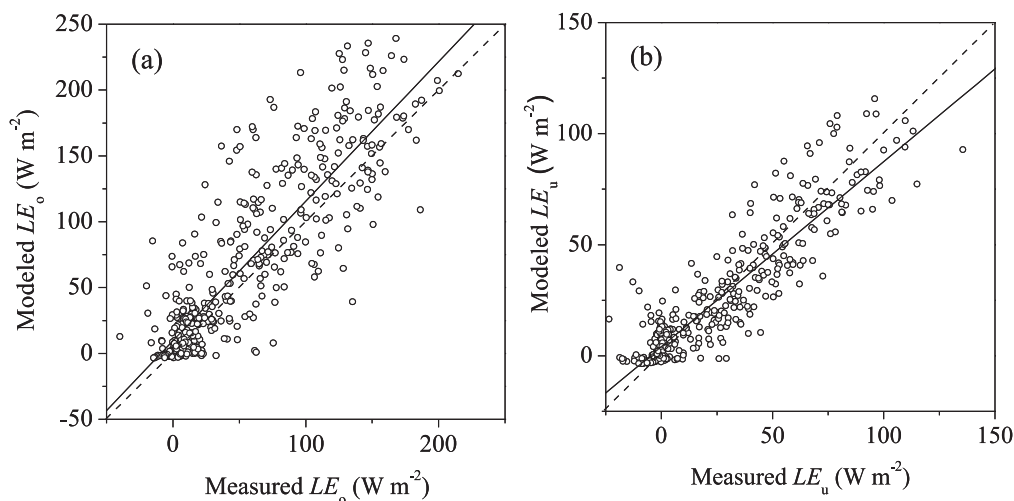


**Fig. 3.** Comparisons between measured and modeled latent heat flux from the above-canopy ( $LE_o$ ) (a) and the understory vegetation ( $LE_u$ ) (b). Solid lines:  $y = 1.06x + 9.61$ ,  $R^2 = 0.75$  for  $LE_o$ ,  $y = 0.83x + 4.11$ ,  $R^2 = 0.83$  for  $LE_u$ . A 1:1 line (broken lines) is also presented.

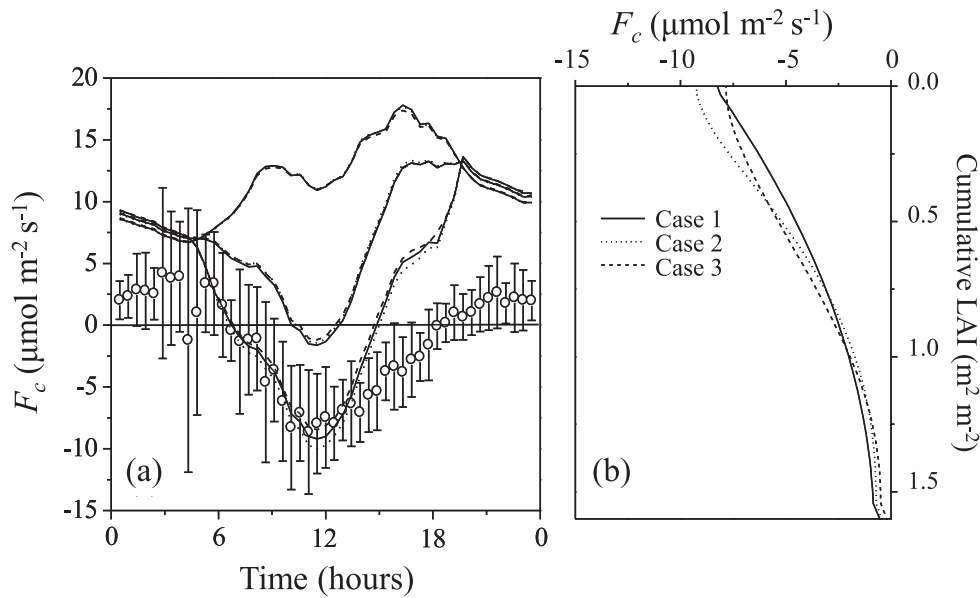


**Fig. 4.** (a) Average temporal variations in measured CO<sub>2</sub> flux ( $F_c$ ) from whole canopy (open circles) and simulated  $F_c$  from whole canopy (lower three lines), understory vegetation (middle three lines) and soil surface (upper three lines) for Cases 1, 2 and 3. For reference, one standard deviation of the measured binned  $F_c$  is also shown. (b) Vertical profiles of the average  $F_c$  around noon (1100–1300 LT) as a function of cumulative leaf area index (LAI) of overstory vegetation modeled from Cases 1, 2 and 3.

For boreal forests, though many studies have their focus upon  $LE_{u_i}$ , few studies have focused upon the  $F_{cu}$ . Kelliher et al. (1999) and Baldocchi and Vogel (1996) measured the  $F_c$  near the forest floor using the eddy covariance method, and detected only positive flux (i.e., soil respiration). This was because there was either no or only sparse understory vegetation at their study sites. In support of this, Siqueira et al. (2003) confirmed that the forest floor was the only CO<sub>2</sub> source in the study site of Kelliher et al. (1999) using an inverse method of the multi-layer turbulent flux model and field measurements. Hollinger et al. (1998) is one of the very few studies that reported a CO<sub>2</sub> sink at the understory vegetation level in a boreal forest. It is noteworthy that, in contrast to the sites of Kelliher et al. (1999) and Baldocchi and Vogel (1996), Hollinger's measurements were conducted in conditions almost identical to our study site, a larch-dominated forest with evergreen shrubs such as cowberry as an understory. The LAI of overstory and understory vegetation in their site was 1.4 and 1.0, respectively, and the peaks

of the  $F_{co}$  and the  $F_{cu}$  were up to  $-5$  and  $-1 \mu\text{mol m}^{-2} \text{s}^{-1}$ , respectively. It is also interesting to compare the proportionality of the  $G_p$  of the understory vegetation to that of the whole canopy, between our study and that of Hollinger et al. (1998). Given the nighttime net ecosystem exchange as the factor of ecosystem respiration in their measurements, the proportionality for this value in their study was about 50%. This is almost identical to our measurement in this study.

**Table 2**

Regression statistics for comparison between the measurements and the numerical experiment results of the above-canopy latent heat ( $LE_o$ ) and CO<sub>2</sub> ( $F_{co}$ ) fluxes for different combinations of leaf area index (LAI) and  $V_{cmax,25}$  profiles.<sup>a</sup>

LAI	$V_{cmax,25}$ profile	Slope	Intercept, $W m^{-2}$	$R^2$	Average, <sup>b</sup> $W m^{-2}$	RMSE, $W m^{-2}$
$LE_o$						
0.5	D <sup>c</sup>	0.89	1.83	0.78	45.83	50.24
	C <sup>d</sup>	0.98	2.18	0.78	50.89	2.63
	D <sup>e</sup>	1.06	9.61	0.75	62.27	166.64
1.6 <sup>e</sup>	C	1.29	9.05	0.76	73.01	764.18
	D	1.23	14.73	0.74	77.56	960.63
3.0	C	1.5	12.61	0.76	86.98	2061.58
LAI	$V_{cmax,25}$ profile	Slope	Intercept, $\mu\text{mol m}^{-2} \text{s}^{-1}$	$R^2$	Average, <sup>b</sup> $\mu\text{mol m}^{-2} \text{s}^{-1}$	RMSE, $\mu\text{mol m}^{-2} \text{s}^{-1}$
$F_{co}$						
0.5	D	0.92	5.08	0.4	3.75	26.97
	C	1.01	4.47	0.43	3.02	18.97
	D <sup>e</sup>	1.07	4.48	0.49	3.29	22.42
1.6 <sup>e</sup>	C	1.44	3.15	0.54	1.14	11.01
	D	1.12	4.35	0.51	2.77	17.9
3.0	C	1.59	2.82	0.55	0.61	11.93

<sup>a</sup> The regression model is  $y = \text{Slope } x + \text{Intercept}$ , where  $y$  and  $x$  are the modeled and measured  $LE_o$  or  $F_{co}$  fluxes, respectively. The coefficient of determination ( $R^2$ ), average ( $W m^{-2}$  for  $LE_o$  and  $\mu\text{mol m}^{-2} \text{s}^{-1}$  for  $F_{co}$ ), and root-mean-squared error (RMSE;  $W m^{-2}$  for  $LE_o$  and  $\mu\text{mol m}^{-2} \text{s}^{-1}$  for  $F_{co}$ ) are also shown.

<sup>b</sup> Averages were calculated from modeled values for a 10-day computation. Averaged values of measured  $LE_o$  and  $F_{co}$  fluxes were  $50.52 W m^{-2}$  and  $-1.32 \mu\text{mol m}^{-2} \text{s}^{-1}$ , respectively.

<sup>c</sup> Decreasing  $V_{cmax,25}$  profile.

<sup>d</sup> Constant  $V_{cmax,25}$  profile.

<sup>e</sup> Cases for model validation.

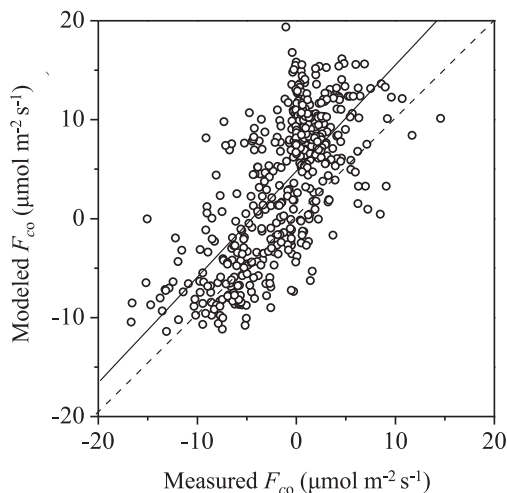


**Fig. 5.** Comparison between measured and modeled CO<sub>2</sub> fluxes from whole canopy ( $F_{co}$ ). Solid line:  $y = 1.07x + 4.82$ ,  $R^2 = 0.49$ . A 1:1 line (broken line) is also presented.

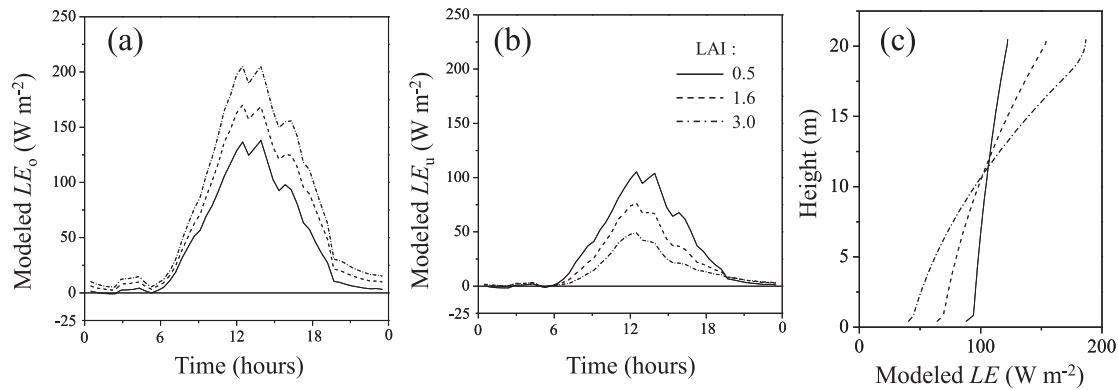


**Fig. 6.** Average temporal variations in modeled latent heat flux from whole canopy (a:  $LE_o$ ) and understory vegetation (b:  $LE_u$ ) and vertical profiles of the average modeled latent heat flux ( $LE$ ) around noon (1100–1300 LT) as a function of canopy height (c), for a larch overstory's leaf area index (LAI) of 0.5, 1.6 and 3.0.

### 3.2. Impact of LAI on flux calculations

An increase in the overstory vegetation's LAI from 0.5 to 3.0 increased the  $LE_o$  in proportion to the increment in the LAI (<3.0) as in the study by Kelliher et al. (1995) (Fig. 6a). Such an increase in the LAI also decreased the  $LE_u$  to the same degree (Fig. 6b). This shows that the increase in  $LE$  from the larch overstory, caused by an increase in its LAI, was about two times that of the decrease in  $LE_u$ . In addition, we found that the gradient of the  $LE$  profile increased with LAI (Fig. 6c). Since this computation assumed the maximum capacity of leaf gas exchange, obtained from the measurements for sunlit leaves of upper and middle part of the canopy, this implies that an ecosystem with a higher LAI has an inefficient leaf gas exchange at the lower part of its canopy. This might cause a near-stable maximum  $LE$  for forests with a high LAI (see Kelliher et al., 1995).

Fig. 7 shows the relationships between  $F_c$  and the overstory vegetation's LAI computed in the same manner as in Fig. 6. The  $F_{co}$  was significantly smaller where the LAI equaled 0.5 than where the LAI equaled 1.6 and 3.0. However, the  $F_{co}$  in the case where the LAI was >1.6 showed little variation (Fig. 7a). On the other hand, an increase in the LAI from 0.5 to 3.0 clearly reduced the  $F_{cu}$  (Fig. 7b). These and further investigations using the  $F_c$  profile as a function of canopy height (Fig. 7c), indicate that when the LAI is >1.6, as was the actual LAI for this site, the increase in larch overstory  $F_c$  compensated for the reduction in cowberry understory  $F_c$ . In this way, a case of constant ecosystem productivity with changing overstory LAI is introduced. Also of note is that a decrease in overstory LAI increases the diurnal range of soil temperature resulting in the fluctuation of  $R_{soil}$ . However, at around noon for this site, this fluctuation in  $R_{soil}$  did not have much affect either upon the  $F_{co}$  or  $F_{cu}$ , while, conversely, it significantly impacted them both in the afternoon (Fig. 7a and b).

In the  $LE$  cases shown in Fig. 6,  $LE_o$  increased with increasing LAI. However, here, when the LAI was >1.6, as was the real LAI in this site, the  $F_{co}$  became saturated. Kumagai et al. (2006) showed that  $F_{co}$  computations were conservative against LAI change within the spatial variation of LAI in a tropical study site. Forest LAI appears to be determined by this maximum and the saturated whole canopy assimilation rate against its water use increase (see Running and Coughlan, 1988).

### 3.3. Impact of leaf physiological traits on flux calculations

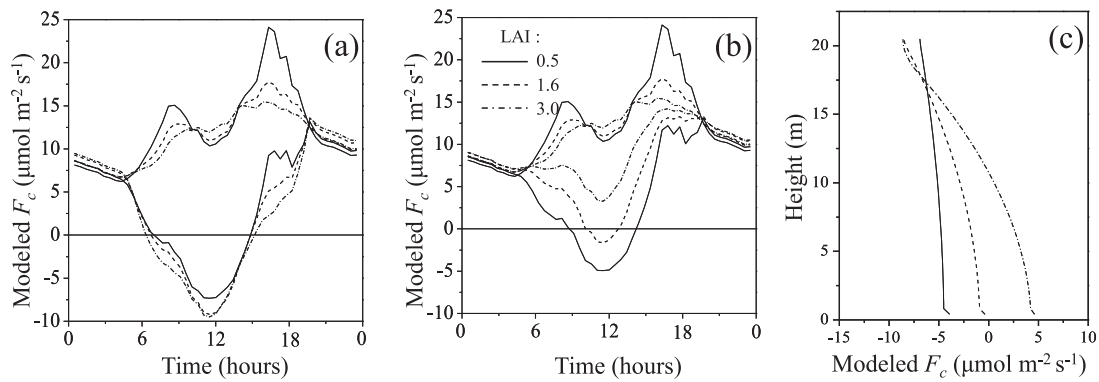
In sparse boreal forest canopies, given the decreasing profile of leaf photosynthetic capacity, i.e.,  $V_{cmax,25}$ , with canopy height decrease, it is instructive to investigate the impacts of both the

$V_{cmax,25}$  profile and the combination of the profile and the LAI on the modeled fluxes. Kumagai et al. (2006) found that in a dense tropical forest canopy, the  $CO_2$  source distribution, calculated on the assumption that  $V_{cmax,25}$  in the canopy top was distributed evenly throughout, was almost the same as that taking the decreasing profile into consideration. Therefore, this resulted in little overall change in  $F_c$ . Thus, the question arises as to whether the result of Kumagai et al. (2006) is applicable to sparse boreal forests. If so, this information might be of use in framing a strategy for measuring the leaf-level physiological parameters required in the construction of the SVAT model, particularly because it is relatively difficult to gain access to some positions within the forest canopy.

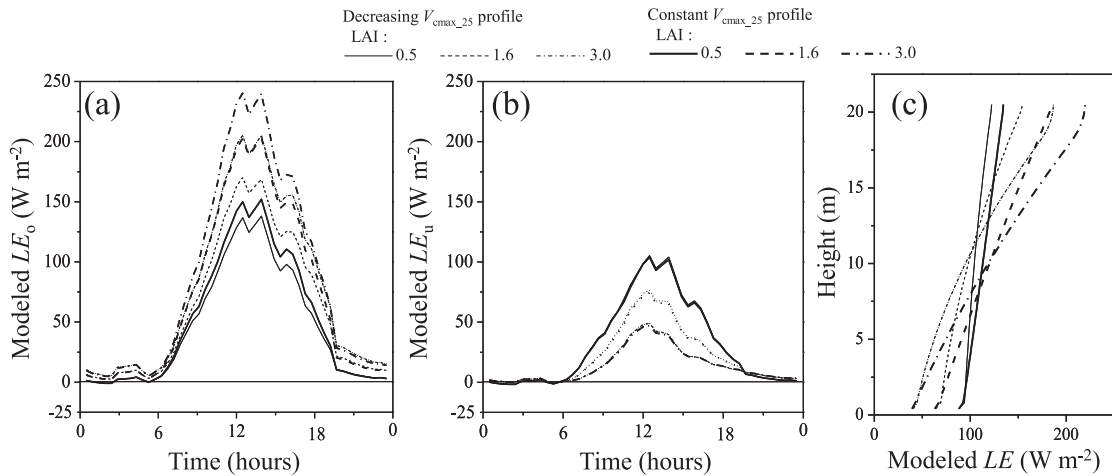
In all overstory LAI cases, modeled  $LE_o$  and  $F_{co}$  were higher for the uniform  $V_{cmax,25}$  profile than for the decreasing  $V_{cmax,25}$  profile. This difference became larger with a larger LAI (Figs. 8 and 9a). As modeled  $LE_u$  and  $F_{cu}$  for all LAI cases were less affected by those  $V_{cmax,25}$  assumptions, this implies that changes in vapor pressure and  $CO_2$  concentration in the within-canopy air, caused by significant changes in the larch overstory's transpiration and assimilation, have little impact on  $LE_u$  (Figs. 8 and 9b). On both  $V_{cmax,25}$  assumptions, the  $LE$  and the  $CO_2$  source strengths at the upper part of the canopy, where the canopy depth from the top is around 7 m (equivalent to 1.0 and 0.5 of the cumulative LAI from the canopy top for the case where LAI equals 3 and 1.6, respectively), were roughly similar at  $10 W m^{-3}$  and  $1.0 \mu mol m^{-3} s^{-1}$ , and  $6 W m^{-3}$  and  $0.7 \mu mol m^{-3} s^{-1}$ , respectively (Figs. 8 and 9c). However, these significantly differed at the lower part of the canopy in each LAI case. This suggests that the reason why source strength in the lower part of the canopy reflects the whole canopy flux is probably because of the effective light attenuation into the lower canopy when the LAI is <3.0 (see Kelliher et al., 1995).

Table 2 summarizes the regression statistics for comparisons between the measurements and the experiment results of  $LE_o$  and  $F_{co}$  for the different combinations of LAI and  $V_{cmax,25}$  profiles. It is interesting that the case for the model validation (i.e., LAI = 1.6 and decreasing  $V_{cmax,25}$  profile) did not show the best fit (small RMSE, slope close to unity, and large  $R^2$ ) between modeled and measured fluxes. However, we emphasize that, when considering the best performance model for both  $LE_o$  and  $LE_u$ , the model validation case reproduced the measurements best (see Figs. 2 and 3). It is clear that both the condition of the increase in LAI and the constant  $V_{cmax,25}$  profile systematically increase the modeled fluxes because those conditions did not impact the  $R^2$  values but increased the slope values (Table 2).

For the most important determinant factor for  $V_{cmax,25}$ ,  $N_a$ , many previous studies have reported, that its decrease with decreasing canopy height is a case of optimal distribution of limited nitrogen



**Fig. 7.** Average temporal variations in modeled CO<sub>2</sub> flux ( $F_c$ ) from whole canopy (lower three lines) and soil surface (=soil respiration: upper three lines) (a) and  $F_c$  from understory vegetation (lower three lines) and soil surface (upper three lines) (b) and vertical profiles of the average modeled  $F_c$  around noon (1100–1300 LT) as a function of canopy height (c), for a larch overstory's leaf area index (LAI) of 0.5, 1.6 and 3.0.



**Fig. 8.** Average temporal variations in modeled latent heat flux from whole canopy (a:  $LE_o$ ) and understory vegetation (b:  $LE_u$ ) and vertical profiles of the average modeled latent heat flux ( $LE$ ) around noon (1100–1300 LT) as a function of canopy height (c), for a larch overstory's leaf area index (LAI) of 0.5, 1.6 and 3 and assuming profiles of constant and decreasing  $V_{cmax,25}$  with decreasing canopy height.

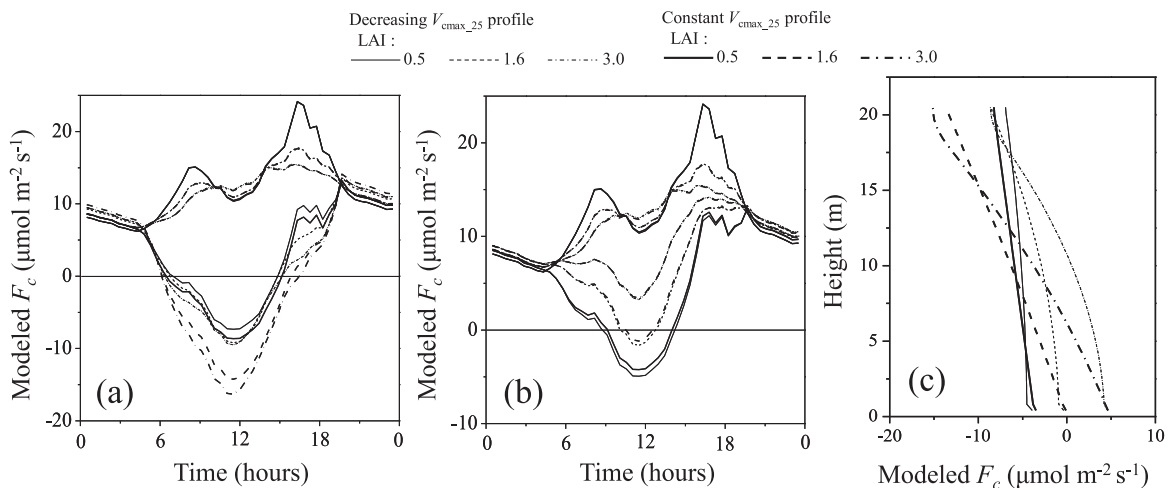


**Fig. 9.** Average temporal variations in modeled CO<sub>2</sub> flux ( $F_c$ ) from whole canopy (a) and  $F_c$  from understory vegetation (b) and vertical profiles of the average modeled  $F_c$  around noon (1100–1300 LT) as a function of canopy height (c), for the larch overstory's leaf area index (LAI) of 0.5, 1.6 and 3 and assuming profiles of constant and decreasing  $V_{cmax,25}$  with decreasing canopy height.

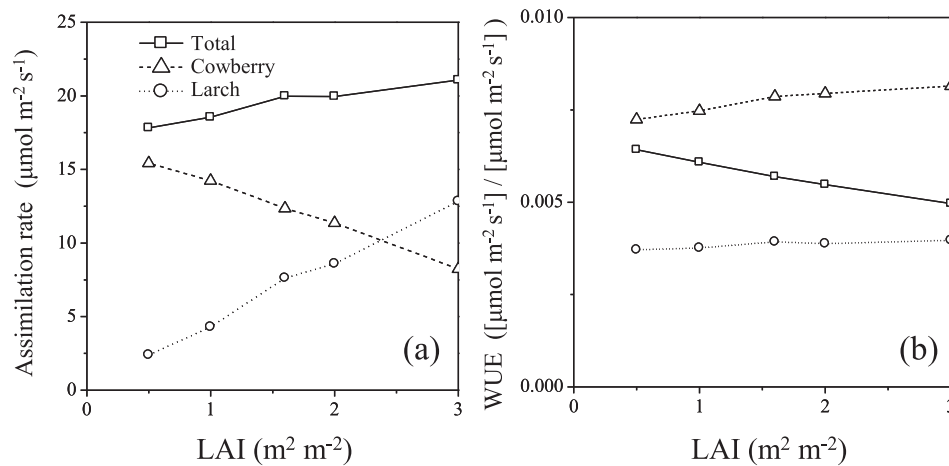


**Fig. 10.** Modeled gross assimilation rate (a) and water use efficiency (b: WUE) averaged around noon (1100–1300 LT) as a function of leaf area index (LAI) of overstory vegetation, for whole canopy (Total), cowberry understory (Cowberry) and larch overstory (Larch).

resources throughout the canopy that does not result in futile nitrogen resources and maximizes the photosynthetic carbon gain (e.g., Hirose and Werger, 1987; Sellers et al., 1992; Kull and Jarvis, 1995; de Pury and Farquhar, 1997). Kumagai et al. (2006) also suggested that for a high LAI forest canopy, having  $N_a$  distributed as much to the upper canopy as to the lower canopy would be futile and provide no benefit for the whole canopy photosynthetic capacity. In other words, for reproducing whole canopy fluxes from a high LAI forest canopy, leaf-level physiological parameters measured from only the upper canopy will be sufficient. However, in this study we found that detailed information on leaf-level physiological traits in the lower canopy are also necessary in computing the transportation of energy and mass between a sparse forest canopy and the atmosphere due to the presence of active exchange in the lower part of the canopy.

#### 3.4. Relationship between productivity partitioning into understory and overstory vegetation and overstory LAI

The  $F_{cu}$  is approximately equivalent to the  $G_p$  of the cowberry understory plus the  $R_{soil}$ , which includes underground biomass respiration for both the cowberry understory and the larch overstory. Hence, using  $G_p$  to compare the productivities of the cowberry and the larch relating to overstory LAI is more favorable than using the  $F_{co}$  and the  $F_{cu}$ . As estimated from Fig. 7, with increasing overstory LAI, the  $G_p$  of the whole canopy remained relatively stable, as that of the larch overstory and cowberry understory increased and decreased, respectively (Fig. 10a). In summary, changes in the overstory LAI does not significantly alter the whole ecosystem's productivity but acts in the partitioning of productivities between the overstory and the understory vegetation. The  $R_{soil}$ , including the heterotrophic respiration and the autotrophic respiration, is divided into those of the larch and the cowberry, the proportions of which may correspond to their biomass. Thus, it is difficult to estimate the net assimilation rates of the larch and cowberry. However, at a LAI of <3.0, the overstory LAI apparently accounted for the coexistence of the larch overstory and the cowberry understory as judged in Fig. 10a.

Since the productivities of the larch, together with that of the whole canopy, increase with increasing overstory LAI (Fig. 10a), it is interesting to question why the larch decreases its LAI resulting in a situation of decreasing productivity and coexistence with the cowberry. Although the larch's water use efficiency (WUE) was relatively constant, the ecosystem WUE decreased with increasing overstory LAI (Fig. 10b). Thus, a decrease in the overstory LAI may

be related to saving the available water resources and thus result in coexistence with the cowberry understory.

Another plausible reason might be that in boreal forests, understory vegetation plays an important role in overstory tree's succession, stand photosynthetic production and nutrient cycling (e.g., George and Bazzaz, 1999; Wardle et al., 2004; Kolari et al., 2006; Hart and Chen, 2008). In particular, in boreal forests, forest fire is one of the major factors affecting the interactions between understory and overstory vegetation communities (see Hart and Chen, 2006). Hart and Chen (2008) suggested that a moderate forest fire may, after initial removal of above-ground vegetation and some of the forest floor, result in the understory vegetation diversity and cover reaching its maximum limit as it responds to the increase in light and nutrient availability. This results in favorable colonizing opportunities for many herbaceous plants and lichens. These opportunities decline with canopy closure and soil nutrient immobilization. Finally, the abundance of species tolerant of low nutrient conditions, e.g., tree species and lichens, increases with declining resource availability. In fact, Isaev and Popov (2007) reported that there were, on average, around 40 forest fires per year near Yakutsk from 1950 to 2005. We therefore presume that, for such ongoing ecosystem processes, overstory vegetation must coexist with understory vegetation (see Wardle et al., 2003).

#### 4. Conclusions

Using a combination of elaborate eddy covariance observations conducted above the forest canopy and at the forest floor, detailed leaf-level physiology measurements (for both overstory and understory vegetation), soil respiration properties measurements, and a multilayer SVAT model, we examined the factors that control the partitioning of whole ecosystem  $LE$  and  $F_c$  into understory and overstory vegetation in a Siberian boreal larch forest. The field data confirmed that the  $LE$  from the cowberry understory vegetation contributed significantly to the whole canopy  $LE$ , and the SVAT model assured that the larch overstory's LAI was a major determinant factor for the flux partitioning of this boreal forest ecosystem. Despite the present comparative unreliability of  $F_c$  measurements, further investigation using the SVAT model implied that the balance of energy exchange and productivity between the larch overstory and the cowberry understory was attributed to the larch overstory's LAI, and that such a balance might be necessary to maintain this boreal larch forest ecosystem. The findings in this study allow us to consider the influence of changes in the within-canopy environment accompanied by forest structural changes

and/or global warming in boreal forest ecosystems. In addition, more extensive and technically difficult experiments are required for below-ground environments such as the examination of the partitioning of root respiration and water uptake between overstory and understory vegetation.

## Acknowledgments

This work was supported by Core Research for Evolutional Science and Technology (CREST) of the Japan Science and Technology Agency (JST), The Global COE (Centers of Excellence) Program (GCOE) of the Japan Society for the Promotion of Science (JSPS) and a grant from the Ministry of Education, Science and Culture of Japan (#20248016). The authors would like to thank the staff of the Institute for Biological Problems of the Cryolithozone, Siberian Division of the Russian Academy of Sciences (RAS), for all their help during the experiment. Tomo'omi Kumagai acknowledges support from the Excellent Young Researcher Overseas Visit Program under the sponsorship of JSPS.

## References

- Badger, M.R., Collatz, G.J., 1977. Studies on the Kinetic Mechanism of Ribulose-1,5-bisphosphate Carboxylase and Oxygenase Reactions, with Particular Reference to the Effect of Temperature on Kinetic Parameters. *Carnegie Institute of Washington Yearbook*, Washington, pp. 355–361.
- Baldocchi, D., Kelliher, F.M., Black, T.A., Paul, J., 2000a. Climate and vegetation controls on boreal zone energy exchange. *Global Change Biol.* 6, 69–83.
- Baldocchi, D., Meyers, T., 1998. On using eco-physiological, micrometeorological and biogeochemical theory to evaluate carbon dioxide, water vapor and trace gas fluxes over vegetation: a perspective. *Agric. Forest Meteorol.* 90, 1–25.
- Baldocchi, D.D., Law, B.E., Anthoni, P.M., 2000b. On measuring and modeling energy fluxes above the floor of a homogeneous and heterogeneous conifer forest. *Agric. Forest Meteorol.* 102, 187–206.
- Baldocchi, D.D., Vogel, C.A., 1996. Energy and CO<sub>2</sub> flux densities above and below a temperate broad-leaved forest and a boreal pine forest. *Tree Physiol.* 16, 5–16.
- Ball, J.T., Woodrow, I.E., Berry, J.A., 1987. A model predicting stomatal conductance and its contribution to the control of photosynthesis under different environmental conditions. In: Biggens, J. (Ed.), *Progress in Photosynthesis Research*. Springer, New York, pp. 221–224.
- Bonan, G.B., 2008. Forests and climate change: forcings, feedbacks, and the climate benefits of forests. *Science* 320, 1444–1449.
- Bonan, G.B., Chapin III, F.S., Thompson, S.L., 1995. Boreal forest and tundra ecosystems as components of the climate system. *Clim. Change* 29, 145–167.
- Bonan, G.B., Pollard, D., Thompson, S.L., 1992. Effects of boreal forest vegetation on global climate. *Nature* 359, 716–718.
- Bousquet, P., Ciais, P., Peylin, P., Ramonet, M., Monfray, P., 1999. Inverse modeling of annual atmospheric CO<sub>2</sub> sources and sinks 1, method and control inversion. *J. Geophys. Res.* 104, 26161–26178.
- Campbell, G.S., Norman, J.M., 1998. *An Introduction to Environmental Biophysics*, 2nd ed. Springer, New York.
- Ciais, P., Tans, P.P., Trolier, M., White, J.W.C., Francey, R.J., 1995. A large northern hemisphere terrestrial CO<sub>2</sub> sink indicated by the <sup>13</sup>C/<sup>12</sup>C ratio of atmospheric CO<sub>2</sub>. *Science* 269, 1098–1102.
- Collatz, G.J., Ball, J.T., Grivet, C., Berry, J.A., 1991. Physiological and environmental regulation of stomatal conductance, photosynthesis and transpiration: a model that includes a laminar boundary layer. *Agric. Forest Meteorol.* 54, 107–136.
- Constantin, J., Grelle, A., Ibrom, A., Morgenstern, K., 1999. Flux partitioning between understory and overstory in a boreal spruce/pine forest determined by the eddy covariance method. *Agric. Forest Meteorol.* 98–99, 629–643.
- de Pury, D.G.G., Farquhar, G.D., 1997. Simple scaling of photosynthesis from leaves to canopies without the errors of big-leaf models. *Plant Cell Environ.* 20, 537–557.
- Dixon, R.K., Brown, S., Houghton, R.A., Solomon, A.M., Trexler, M.C., Wisniewski, J., 1994. Carbon pools and flux of global forest ecosystems. *Science* 263, 185–190.
- Dolman, A.J., Maximov, T.C., Moors, E.J., Maximov, A.P., Elbers, J.A., Kononov, A.V., et al., 2004. Net ecosystem exchange of carbon dioxide and water of far eastern Siberian Larch (*Larix cajanderii*) on permafrost. *Biogeosciences* 1, 133–146.
- Farquhar, G.D., von Caemmerer, S., Berry, J.A., 1980. A biochemical model of photosynthetic CO<sub>2</sub> assimilation in leaves of C<sub>3</sub> species. *Planta* 149, 78–90.
- Farquhar, G.D., Wong, S.C., 1984. An empirical model of stomatal conductance. *Aust. J. Plant Physiol.* 11, 191–210.
- Food and Agriculture Organization, 2005. *State of the World's Forests 2005*. Food and Agriculture Organization of the United Nations, Forest Department, Rome.
- George, L.O., Bazzaz, F.A., 1999. The fern understory as an ecological filter: growth and survival of canopy-tree seedlings. *Ecology* 80, 846–856.
- Goudriaan, J., 1977. *Crop Micrometeorology: A Simulation Study*. Centre for Agricultural Publishing, Documentation, Wageningen.
- Hamada, S., Ohta, T., Hiyama, T., Kuwada, T., Takahashi, A., Maximov, T.C., 2004. Hydrometeorological behaviour of pine and larch forests in eastern Siberia. *Hydrol. Process.* 18, 23–39.
- Hart, S.A., Chen, H.Y.H., 2006. Understory vegetation dynamics of North American boreal forests. *Crit. Rev. Plant Sci.* 25, 381–397.
- Hart, S.A., Chen, H.Y.H., 2008. Fire, logging, and overstory affect understory abundance, diversity, and composition in boreal forest. *Ecol. Monogr.* 78, 123–140.
- Hirose, T., Werger, M.J.A., 1987. Maximizing daily canopy photosynthesis with respect to the leaf nitrogen allocation pattern in the canopy. *Oecologia* 72, 520–526.
- Hollinger, D.Y., Kelliher, F.M., Schulze, E.D., Bauer, G., Arneth, A., Byers, J.N., et al., 1998. Forest-atmosphere carbon dioxide exchange in eastern Siberia. *Agric. Forest Meteorol.* 90, 291–306.
- Iida, S., Ohta, T., Matsumoto, K., Nakai, T., Kuwada, T., Kononov, A.V., et al., 2009. Evapotranspiration from understory vegetation in an eastern Siberian boreal larch forest. *Agric. Forest Meteorol.* 149, 1129–1139.
- Isaev, A.S., Popov, V.F., 2007. The reconstruction of forest fire history in Central Yakutia, Eastern Siberia. In: Ohta, T., Maximov, T.C., Dolman, H. (Eds.), *Proceedings of 3rd International WS on C/H<sub>2</sub>O/Energy Balance and Climate over Boreal Regions with Special Emphasis on Eastern Eurasia*. Japan Science and Technology Agency, Nagoya, p. 89.
- Jarvis, P.G., Saugier, B., Schulze, E.D., 2001. Productivity of boreal forests. In: Roy, J., Saugier, B. (Eds.), *Terrestrial Global Productivity*. Academic Press, San Diego.
- Katul, G.G., Albertson, J.D., 1998. An investigation of higher-order closure models for a forested canopy. *Boundary Lay. Meteorol.* 89, 47–74.
- Katul, G.G., Albertson, J.D., 1999. Modeling CO<sub>2</sub> sources, sinks, and fluxes within a forest canopy. *J. Geophys. Res.* 104, 6081–6091.
- Kelliher, F.M., Hollinger, D.Y., Schulze, E.D., Vygodskaya, N.N., Byers, J.N., Hunt, J.E., et al., 1997. Evaporation from an eastern Siberian larch forest. *Agric. Forest Meteorol.* 85, 135–147.
- Kelliher, F.M., Leuning, R., Raupach, M.R., Schulze, E.D., 1995. Maximum conductances for evaporation from global vegetation types. *Agric. Forest Meteorol.* 73, 1–16.
- Kelliher, F.M., Lloyd, J., Arneth, A., Byers, J.N., McSeveny, T.M., Milukova, I., et al., 1998. Evaporation from a central Siberian pine forest. *J. Hydrol.* 205, 279–296.
- Kelliher, F.M., Lloyd, J., Arneth, A., Lühker, B., Byers, J.N., McSeveny, T.M., et al., 1999. Carbon dioxide efflux density from the floor of a central Siberian pine forest. *Agric. Forest Meteorol.* 94, 217–232.
- Kolari, P., Pumpanen, J., Kulmala, L., Ilvesniemi, H., Nikinmaa, E., Grönholm, T., et al., 2006. Forest floor vegetation plays an important role in photosynthetic production of boreal forests. *Forest Ecol. Manage.* 221, 241–248.
- Kononov, A.V., Maximov, T.C., Suzdalov, D.A., Moors, E., 2006. Seasonal trends of soil respiration in taiga permafrost region of Central Yakutia. In: Dolman, H., Moors, E., Ohta, T., Maximov, T.C. (Eds.), *International Workshop on H<sub>2</sub>O and CO<sub>2</sub> Exchange in Siberia*. Japan Science and Technology Agency, Nagoya, pp. 49–52.
- Kull, O., Jarvis, P.G., 1995. The role of nitrogen in a simple scheme to scale up photosynthesis from leaf to canopy. *Plant Cell Environ.* 18, 1174–1182.
- Kumagai, T., Ichie, T., Yoshimura, M., Yamashita, M., Kenzo, T., Saitoh, T.M., et al., 2006. Modeling CO<sub>2</sub> exchange over a Bornean tropical rain forest using measured vertical and horizontal variations in leaf-level physiological parameters and leaf area densities. *J. Geophys. Res.* 111, D10107, doi:10.1029/2005JD006676.
- Maksimov, A., Karsanaev, S., Kruij, B., Jans, W., Kononov, A., Maximov, T.C., Moors, E., Saito, H., 2006. A/C<sub>1</sub> curve analysis of *Larix cajanderii* growing in Central Yakutia, Siberia. In: Dolman, H., Moors, E., Ohta, T., Maximov, T.C. (Eds.), *International Workshop on H<sub>2</sub>O and CO<sub>2</sub> Exchange in Siberia*. Japan Science and Technology Agency, Nagoya, pp. 57–60.
- Malhi, Y., Baldocchi, D.D., Jarvis, P.G., 1999. The carbon balance of tropical, temperate and boreal forests. *Plant Cell Environ.* 22, 715–740.
- Matsumoto, K., Ohta, T., Nakai, T., Kuwada, T., Daikoku, K., Iida, S., et al., 2008. Energy consumption and evapotranspiration at several boreal and temperate forests in the Far East. *Agric. Forest Meteorol.* 148, 1978–1989.
- Mellor, G.L., 1973. Analytic prediction of the properties of stratified planetary surface layers. *J. Atmos. Sci.* 30, 1061–1069.
- Nakai, T., Sumida, A., Daikoku, K., Matsumoto, K., van der Molen, M.K., Kodama, Y., et al., 2008. Parameterisation of aerodynamic roughness over boreal, cool- and warm-temperate forests. *Agric. Forest Meteorol.* 148, 1916–1925.
- Nakai, T., Van Der Molen, M.K., Gash, J.H.C., Kodama, Y., 2006. Correction of sonic anemometer angle of attack errors. *Agric. Forest Meteorol.* 136, 19–30.
- Niinemetts, U., Tenhunen, J.D., 1997. A model separating leaf structural and physiological effects on carbon gain along light gradients for the shade-tolerant species. *Plant Cell Environ.* 20, 845–866.
- Ohta, T., Hiyama, T., Tanaka, H., Kuwada, T., Maximov, T.C., Ohata, T., et al., 2001. Seasonal variation in the energy and water exchanges above and below a larch forest in eastern Siberia. *Hydrol. Process.* 15, 1459–1476.
- Ohta, T., Maximov, T.C., Dolman, A.J., Nakai, T., van der Molen, M.K., Kononov, A.V., et al., 2008. Interannual variation of water balance and summer evapotranspiration in an eastern Siberian larch forest over a 7-year period (1998–2006). *Agric. Forest Meteorol.* 148, 1941–1953.
- Pattey, E., Strachan, I.B., Desjardins, R.L., Massheder, J., 2002. Measuring nighttime CO<sub>2</sub> flux over terrestrial ecosystems using eddy covariance and nocturnal boundary layer methods. *Agric. Forest Meteorol.* 113, 145–158.

- Rödenbeck, C., Houweling, S., Gloor, M., Heimann, M., 2003. CO<sub>2</sub> flux history 1982–2001 inferred from atmospheric data using a global inversion of atmospheric transport. *Atmos. Chem. Phys.* 3, 1919–1964.
- Running, S.W., Coughlan, J.C., 1988. A general model of forest ecosystem processes for regional applications I. Hydrologic balance, canopy gas exchange and primary production processes. *Ecol. Model.* 42, 125–154.
- Sellers, P.J., Berry, J.A., Collatz, G.J., Field, C.B., Hall, F.G., 1992. Canopy reflectance, photosynthesis, and transpiration. III. A reanalysis using improved leaf models and a new canopy integration scheme. *Remote Sens. Environ.* 42, 187–216.
- Siqueira, M., Leuning, R., Kolle, O., Kelliher, F.M., Katul, G.G., 2003. Modelling sources and sinks of CO<sub>2</sub>, H<sub>2</sub>O and heat within a Siberian pine forest using three inverse methods. *Q. J. R. Meteorol. Soc.* 129, 1373–1393.
- Snyder, P.K., Delire, C., Foley, J.A., 2004. Evaluating the influence of different vegetation biomes on the global climate. *Clim. Dyn.* 23, 279–302.
- Tans, P.P., Fung, I.Y., Takahashi, T., 1990. Observational constraints on the global atmospheric CO<sub>2</sub> budget. *Science* 247, 1431–1438.
- von Caemmerer, S., Evans, J.R., Hudson, G.S., Andrews, T.J., 1994. The kinetics of ribulose-1,5-bisphosphate carboxylase/oxygenase in vivo inferred from measurements of photosynthesis in leaves of transgenic tobacco. *Planta* 195, 88–97.
- von Caemmerer, S., Farquhar, G.D., 1981. Some relationships between the biochemistry of photosynthesis and the gas exchange of leaves. *Planta* 153, 376–387.
- Wardle, D.A., Bardgett, R.D., Klironomos, J.N., Setälä, H., Van Der Putten, W.H., Wall, D.H., 2004. Ecological linkages between aboveground and belowground biota. *Science* 304, 1629–1633.
- Wardle, D.A., Hornnberg, G., Zackrisson, O., Kalela-Brundin, M., Coomes, D.A., 2003. Long-term effects of wildfire on ecosystem properties across an island area gradient. *Science* 300, 972–975.
- Watanabe, T., 1993. The bulk transfer coefficients over a vegetated surface based on K-theory and a 2nd-order closure model. *J. Meteorol. Soc. Jpn.* 71, 33–42.
- Webb, E.K., Pearman, G.I., Leuning, R., 1980. Correction of flux measurements for density effects due to heat and water vapour transfer. *Q. J. R. Meteorol. Soc.* 106, 85–100.
- Wilson, N.R., Shaw, R.H., 1977. A higher order closure model for canopy flow. *J. Appl. Meteorol.* 16, 1197–1205.
- Wullschlegel, S.D., 1993. Biochemical Limitations to carbon assimilation in C<sub>3</sub> plants – a retrospective analysis of the A/C<sub>i</sub> curves from 109 species. *J. Exp. Bot.* 44, 907–920.